JOURNAL OF Applied Polymer SCIENCE

Ethylene-Methyl Acrylate-Glycidyl Methacrylate Toughened Poly(lactic acid) Nanocomposites

Touffik Baouz,[1] Farouk Rezgui,[1] Ulku Yilmazer[2]

[1]Laboratoire des Matériaux Organiques, Faculté de Technologie, Département de Génie des Procédés, Université Abderrahmane Mira, Béjaia 06000, Algeria

[2]Chemical Engineering Department, Middle East Technical University, 06800, Ankara, Turkey

Correspondence to: T. Baouz (E-mail: baouztoufik@yahoo.fr)

ABSTRACT: Poly (lactic acid) (PLA) was melt blended in a twin screw extruder using an ethylene-methyl acrylate-glycidyl methacrylate rubber as a toughener. PLA/rubber blends were immiscible as observed by scanning electron microscopy. Impact strength and ductility of PLA were improved by the addition of the rubber at the expense of strength and stiffness. An organo-montmorillonite (OMMT) was used at 2 wt % to counteract the negative effect of the rubber on modulus, and balanced properties were observed at 10 wt % rubber content. X-ray diffraction and transmission electron microscopy revealed the formation of intercalated/exfoliated structure in the ternary nanocomposites. Thermal behavior analysis indicated that the degree of crystallinity is slightly affected by the clay and the rubber. Both the clay and the rubber decreased the crystallization temperature of PLA and acted as nucleating agents for PLA. The viscosity of the mixtures as measured by melt flow index was highly influenced by the rubber and the OMMT. © 2012 Wiley Periodicals, Inc. J. Appl. Polym. Sci. 000: 000–000, 2012

KEYWORDS: Poly(lactic acid); nanocomposite; organoclay; rubber toughening; glycidyl methacrylate

Received 19 April 2012; accepted 19 August 2012; published online
DOI: 10.1002/app.38529

INTRODUCTION

Biodegradable polymers play a major role in the protection of the environment by reducing the amount of wastes derived from petroleum based polymers, and they limit the depletion of natural resources that are finite. Among a number of bio-based polymers, poly (lactic acid) produced from renewable resources is a linear aliphatic thermoplastic polyester with promising potential to substitute for conventional polymers owing to its biodegradability, renewability, processability, and climate-naturality.[1,2]

PLA found use in diverse applications such as in biomedical and packaging fields.[2,3] Although PLA has comparable properties to many conventional polymers, its brittleness and low glass transition temperature hindered its applications where toughness is desired. To overcome this limitation various strategies have been adopted such as copolymerization, plasticization, addition of organic/inorganic fillers, and melt-blending with either biodegradable or nonbiodegradable polymers.[2–4]

It is proposed that improvement of several mechanical properties are possible by copolymerization; however, up to now none of the PLA copolymers are reported to be economically feasible or commercially available.[5,6] Plasticizers are used to enhance ductility and flexibility, but researchers are faced with two major issues: evaporation of small-sized plasticizers during processing at elevated temperatures and migration of the plasticizers to the surface of the polymer matrix.[7,8] As rigid fillers, metal oxides,[9] calcium carbonate,[10] hydroxyapetite,[11] and organically modified clays were investigated.[12,13] Organically modified layered silicates are favored since their high aspect ratio was shown to bring superior mechanical, rheological, fire retardancy, and gas barrier properties.[14–16] In most cases, addition of layered silicates is known to increase rigidity, but decrease toughness. Chang et al.[17] prepared nanocomposites using a montmorillonite modified with hexadecylamine (C_{16}-MMT) and a fluorinated-mica modified with hexadecylamine (C_{16}-Mica) via solution intercalation. The maximum ultimate tensile strength was observed at a certain clay concentration (4 wt %) for both types of fillers. Furthermore, in C_{16}-MMT, the initial modulus increased with increasing organoclay content up to the same critical clay concentration.

Melt blending with various polymers is the mostly preferred strategy in toughening PLA. Numerous biodegradable polymers were reported to have been melt blended with PLA to enhance toughness.[2,18] Among the biodegradable ones, polycaprolactone (PCL) is one of the most extensively investigated polymers.

However, it is immiscible with PLA, hence it requires compatibilizers. Broz et al.[19] produced binary blends of PLA/PCL and obtained an increase in strain at break above a PCL content of 60 wt %, accompanied by reduction in tensile modulus and strength. On the other hand, addition of a small amount of PLA–PCL–PLA triblock copolymer (4 wt %) to PLA/PCL binary blends improved the dispersion of PCL in PLA and enhanced the ductility. PLA was also toughened with miscellaneous nonbiodegradable polymers such as Linear Low Density Polyethylene[20] Polycarbonate[21] and Poly(Ethylene Oxide).[22]

Addition of suitable rubbery polymer is an effective way to enhance toughness, since the rubber blended with the brittle polymer dissipates the stress so that the material shows ductility and plastic deformation. Among the factors governing the performance of rubber toughened polymers the rubber content, rubber domain size and distribution, interfacial tension and viscosity ratio between the polymer matrix and the rubber can be cited.[23,24] The main toughening mechanisms responsible for energy dissipation resulting in enhanced properties include crazing and shear yielding of the polymer matrix and cavitation of the rubber inclusions.[2,25]

Numerous research studies have been published where biodegradable[3,26] and nonbiodegradable rubbers[27–30] were used to toughen PLA. Sun et al.[4] synthesized glycidyl methacrylate (GMA) functionalized acrylonitrile-butadiene-styrene (ABS-*g*-GMA) by emulsion polymerization at different concentrations of GMA and used them to improve the toughness of PLA. The reaction of the epoxy groups of ABS-*g*-GMA and carboxyl and hydroxyl terminal groups of PLA was observed by torque measurements. These reactions are schematically shown in Reference 4. Hashima et al.[31] improved the impact strength and elongation at break of PLA by the addition of hydrogenated styrene-butadiene-styrene block copolymer (SEBS) rubber to PLA, and further enhancement was observed by using poly (ethylene-glycidyl-methacrylate) EGMA as a compatibilizer. Oyama[28] studied a reactive blend of PLA with EGMA rubber. The reported Charpy impact strength (72 KJ/m^2) for the blend (80/20, w/w) was 50 times higher than that of the pristine PLA after annealing the samples at 90°C for 2.5 h.

Production of ternary nanocomposites for combining the advantages of layered silicates and rubbers is another alternative to improve the properties of PLA. Recently PLA/organo-montmorillonite (PLA/OMMT) toughened with maleated styrene-ethylene-butylene-styrene (SEBS-*g*-MAH) was studied by Leu et al.[29] It was reported that some of the clay was encapsulated into the rubber phase owing to its affinity to the maleic anhydride groups of the rubber. It was also observed that the degree of crystallinity decreased with increasing rubber content and both elongation and tensile impact strength were improved at the expense of modulus and strength. Bitinis et al.[32] toughened PLA with natural rubber (NR) using three different nanoclays. The two organo-montmorillonites were observed to be located at the interface and they acted as compatibilizer and barrier for coalescence of the rubbery phase, resulting in finer particle dispersion of the rubber. However, the unmodified clay resided in the PLA matrix and did not affect the NR droplet morphology. PLA rubber toughened blends are rather well documented, but the literature on their ternary nanocomposites is scarce.

The objective of this work was an attempt to toughen PLA with an ethylene-methyl acrylate-glycidyl methacrylate (E-MA-GMA) rubber by reactive blending in a twin screw extruder. To counterbalance the loss in modulus of these blends, an organo-montmorillonite clay was used to prepare ternary nanocomposites. The structure of the materials was investigated by XRD, TEM, and SEM. Thermal properties of the materials were studied by DSC, and their mechanical performance was evaluated by impact and tensile testing. Melt Flow Index (MFI) measurements were carried out to determine the rheological properties of the mixtures.

EXPERIMENTAL

Materials

PLA (PLI 005) of commercial injection grade was obtained from NaturePlast (Caen, France). According to the manufacturer, it has a density of 1.25 g/cm^3 (ISO 1183), and a melting temperature in the range of 145–155°C. The rubber, Lotader® AX8900 was obtained from ARKEMA (Puteaux, France). It is a terpolymer of ethylene-methyl acrylate and glycidyl-methacrylate (E-MA-GMA). According to the data sheet of the material, methyl acrylate and GMA contents are 24 and 8 wt % respectively. The nanoscale filler was an organo-modified montmorillonite clay, Closite® 30B, provided by Southern Clay Products (Gonzales, Texas, USA). The cation of the organic modifier of the clay is methyl, tallow, bis-2-hydroxyethyl, quaternary ammonium (MT2EtOH) used at a concentration of 90 mEq/100 g clay, and the anion is chloride.

Preparation of the Samples

Before the extrusion step, PLA and organoclay were dried overnight at 80°C in a vacuum oven and the rubber was dried overnight at 45°C in a conventional oven. In the binary and ternary nanocomposites, the weight percent of the rubber was varied in the range of 5–30 wt %, and the amount of clay in the nanocomposites was kept constant at 2 wt %. All the mixtures were prepared using a Thermoprism TSE 16 TC fully intermeshing, co-rotating twin screw extruder ($L/D = 24$) with processing zone temperatures of 150–170–170–170–170°C from the hopper to the die. The dry mixtures were tumbled in a plastic bag and fed directly into the hopper equipped with a mixer. The screw speed was 250 rpm and the feed rate was 25 g/min.

The extruded rods were collected on aluminum plates and cooled at ambient temperature to avoid hydrolysis of PLA by water cooling. Thereafter, a pelletizer was used to grind the extrudates. For comparison, PLA was extruded at the same conditions as for the blends and nanocomposites to serve as reference.

Specimens for characterization tests were prepared using a DSM Xplore mini injection molding equipment at cylinder and mold temperatures of 170 and 60°C, respectively. Prior to injection molding, all materials were dried overnight in a vacuum oven at 80°C.

CHARACTERIZATION

X-Ray Diffraction (XRD) and Transmission Electron Microscopy (TEM)

The nanocomposite samples for XRD tests were cut from dog-bone tensile bars. X-ray diffraction (XRD) measurements were performed at room temperature in the reflection mode for the organoclay pristine powder and the molded nanocomposites using a Rigaku D/MAX 2200/PC X-ray diffractometer. A monochromatic CuKα radiation ($\lambda = 1.5418$ Å), that generated a voltage of 40 kV and current of 40 mA, was used as a source. X-ray patterns were recorded with a step size of 0.02° from $2\theta = 1°$ to 10° at 1°/min scan rate. The basal spacing or (d_{001}) reflection of the samples was calculated from the peak positions using Bragg's law.

The microstructure of the nanocomposites was observed using a FEI Spirit G^2 Biotwin transmission electron microscope under an accelerating voltage of 80 kV in bright field mode. Ultrathin sections (70–80 nm) of the nanocomposites were obtained from impact test bars with Leica Ultracut UCT Ultramicrotome and deposited onto copper grids.

Scanning Electron Microscopy

Scanning electron microscopy (SEM) observations were made on cryofractured specimens. Injection molded impact test bars were immersed and kept in liquid nitrogen for 5 min and then broken. Etching of the rubber phase was carried out in a sonication bath at 45°C with liquid n-heptane until the surface of the specimen was whitened. The etched cryofractured surfaces were coated with thin gold film and analyzed with a Jeol JSM-6400 low voltage microscope. Domain size of the dispersed rubber phase in the prepared materials was determined by using ImageJ software program.[33]

Mechanical Properties

The mechanical tests were performed at room temperature. The tensile modulus, tensile strength, and elongation at break were obtained through tensile tests carried out according to ISO 527 using a Shimadzu Autograph AG-IS 100 KN dynamometer at a crosshead speed of 3 mm/min. Notched Charpy impact strength measurements were done by using a Ceast Resil Impactor pendulum according to ISO 179. The notch had a radius of 0.1°, an angle of 45°, and a depth of 2 mm. In both tests, at least five specimens were tested for each set of samples, and the mean value and the standard deviations are reported.

Melt Flow Index Measurements

Melt flow index (MFI) of the neat components and the mixtures was measured according to ISO 1133 using Omega Melt Flow Indexer at a temperature of 190°C under a load of 2.16 kg. At least five measurements were taken for each sample and the results were averaged to obtain a mean value.

Thermal Properties

Thermal behavior of the materials was studied using DSC-60 Shimadzu Differential Scanning Calorimetry (DSC). Samples of 9–10 mg were cut from injection molded tensile bars, sealed in aluminum pans and heated from room temperature to 220°C at a heating rate of 10°C/min under nitrogen purge to avoid moisture and oxidative degradation. The glass transition temperature (T_g), crystallization temperature (T_c), melting temperature (T_m), crystallization enthalpy (ΔH_c), and melting enthalpy (ΔH_m) were determined from this scan. The degree of crystallinity of PLA in the compounds was estimated using the following equation:

$$W_c(\%) = \left(\frac{\Delta H_m - \Delta H_c}{\Delta H_f \times \emptyset_{PLA}}\right) \times 100 \quad (1)$$

where $W_c(\%)$ is the degree of crystallinity, ΔH_m and ΔH_c are the heats of fusion and crystallization of the sample respectively, ΔH_f is the heat of fusion of 100% crystalline PLA, and $\emptyset_{PLA}$ is the weight fraction of the PLA in the sample.

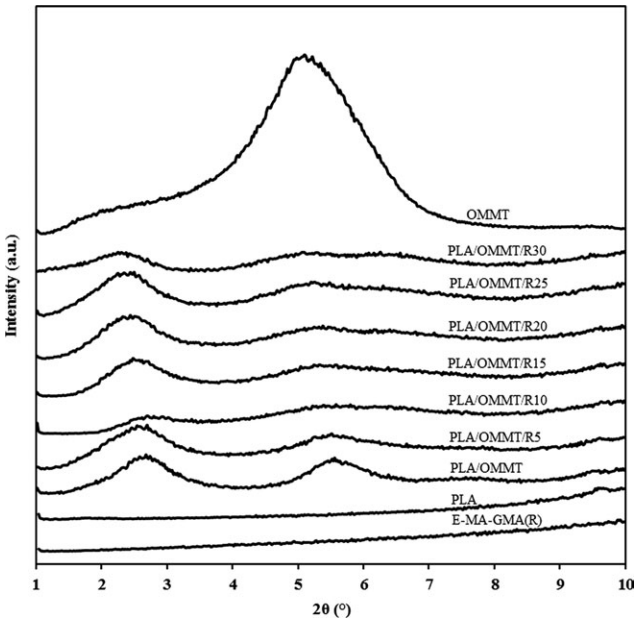

Figure 1. X-Ray patterns of PLA, rubber and the nanocomposites at 2 wt % OMMT. (The R indicates the rubber, and the number following R indicates the wt % of the rubber). The curves are shifted vertically for clarity.

RESULTS AND DISCUSSION

XRD Analyses

The structure of a nanocomposite, i.e. the extent of intercalation and exfoliation govern its properties. Thus, it is of paramount importance to determine the degree to which polymers intercalate the silicate sheets of the clay. TEM and XRD techniques have been widely used to evaluate the dispersion state of the clay platelets in polymer/clay nanocomposites.[2,12,15] The structure of a nanocomposite is usually established using XRD analysis at low angles ($2\theta < 10°$).[2,14,15] The interlayer spacing, called also "*d*-spacing", of the clay platelets can be evaluated from the primary diffraction peak position of the organoclay in the XRD diffractogram and Bragg's law ($n\lambda = 2\ d\ \sin\theta$). The disappearance of the characteristic peak, its shift to lower diffraction angle and the broadening of the peak suggest exfoliation, intercalation, and partial exfoliation respectively.[34]

Figure 1 shows the XRD traces recorded for PLA/OMMT and PLA/OMMT/rubber nanocomposites. XRD diffractograms of

OMMT, PLA, and rubber are also presented for comparison. The OMMT weight fraction in the nanocomposites was maintained constant at 2 wt %. PLA and the rubber displayed no characteristic peak in the range of observation, while the reference diffractogram of OMMT clay in pure powder form exhibited a strong peak at a diffraction angle of ($2\theta = 5.1°$), which corresponds to an interlayer spacing of 1.73 nm. This value corroborates with that reported in the manufacturer's data sheet.

When compounded with PLA, the characteristic diffraction peak of the organoclay shifted to lower diffraction angle ($2\theta = 2.58°$) and the intensity decreased suggesting that the *d*-spacing (d_{001}) increased to 3.42 nm. The distance between the clay platelets in the binary PLA/OMMT nanocomposite is larger than that in the neat clay indicating intercalation. The intercalated structure might be attributed to the affinity of PLA to the organoclay through hydrogen bonding between the carboxyl and hydroxyl end groups of PLA with the surface of OMMT and to possible interactions that might have also occurred between the terminal carboxyl groups of PLA with the hydroxyl groups of the surfactant present in the OMMT.[20] The original peak of the clay still appears in the diffractogram of this nanocomposite with lower intensity suggesting that some of the clay layers were not intercalated.

Addition of 5 wt % rubber to PLA/OMMT did not significantly affect the structure of the nanocomposite (Figure 1). As it can be observed, the original peak of the organoclay at ($2\theta = 5.1°$) still exists, but is smaller and broader implying intercalation and partial exfoliation due to additional intercalation of the rubber between the galleries of the clay. When the rubber content was increased to 10 wt %, both peaks disappeared from the diffractogram indicating complete exfoliation of the organoclay. This may be attributed to the affinity of the reactive rubber to the modifier of the clay. The rubber contains glycidyl reactive groups and ester moieties that might have interacted with both the clay modifier and PLA. In this sense, the rubber modifier also played the role of a compatibilizer and promoted dispersion of the OMMT.[15,34] Similar results were obtained by Chow et al.[14] In their study, they reported an incremental increase in the d-spacing when EPM-g-MAH was added to the PLA/OMMT system that was attributed to the diffusion of the rubber into the galleries of clay. Furthermore, addition of the rubber increased the shear intensity applied on the clay during processing owing to its high viscosity. Hence, more clay platelets were delaminated and dispersion and intercalation were improved.[34]

Except for the 10 wt % rubber content, it can be seen that the original peak of the clay still existed with a slight shift to lower angle, but it became broader and decreased in intensity, implying the presence of ordered tactoids.[34] It should be noted that at 10 wt % rubber content, an optimum balance of the mechanical properties was obtained. Beyond 10 wt % rubber content, the two peaks reappeared at approximately the same diffraction angles ($2\theta = 2.44°$) and ($2\theta = 5.08°$) corresponding to basal spacings of 3.62 nm and 1.74 nm, respectively, and no further enhancement was observed in the intercalation/exfoliation process. This might be explained by the competitive interaction between the PLA and the rubber, in comparison to that between the polymers and the clay. Another possibility is that the rubber might have bonded to the edges of the clays through interactions of the hydroxyl groups of the clay and no further penetration into the clay galleries took place.

TEM Analyses

XRD results do not give complete information about the spatial distribution of the clay. Thus, TEM is generally used as a complementary technique to get a direct visualization of the dispersion state in the nanocomposites.[2,15,34] Typical TEM micrographs of the nanocomposites are shown in Figure 2. The TEM micrographs reveal the formation of nanocomposites that corroborate with the XRD results discussed earlier. The dark bundles and ribbons represent the clay particles and the light grey areas show the polymer matrix.

Figure 2(a) is a TEM micrograph of binary PLA/OMMT at low magnification illustrating that the clay nanoplatelets were dispersed quite homogeneously. Figure 2(b) exhibits the formation of intercalated/exfoliated structure in the binary PLA/OMMT nanocomposite, and Figure 2(c) displays the TEM image of the ternary nanocomposite with 10 wt % rubber content. Isolated exfoliated platelets, intercalated clay and small tactoids can be clearly observed in Figures 2(b, c). All of the ternary nanocomposites exhibited partial exfoliation, intercalation and small tactoids. It is also clearly observed from Figure 2(d–f) that addition of more rubber did not further improve exfoliation. These observations are consistent with the results of XRD analysis.

It is reported that the location of the clay in a rubber toughened nanocomposite affects the particle size of the dispersed phase and thus the performance of the mixture. There are controversial reports on the effects of organoclay location on toughness in rubber toughened nanocomposites. Some reports point out that the highest toughness was achieved when the clay was dispersed in the continuous phase, whereas others claim that the highest improvement in toughness was obtained when the clay was at the interface or dispersed inside the minor phase.[35]

It was not possible to determine the position of the clay particles in the mixtures by the TEM micrographs owing to the low contrast difference between the PLA and the rubber. Clay particles are more likely to be located in the PLA matrix, since it is more polar than the rubber, and it has lower viscosity than the rubber. However, scanning electron microscopy and mechanical properties analyses that are discussed later suggest that most of the clay particles might be embedded in the rubber phase and some were located at the interface of the rubber and PLA as well as in the PLA matrix. This could be due to the fact that during melt compounding, the rubber melted first ($T_m \approx 53°C$) and encapsulated most of the clay before PLA started melting at ~152°C.

SEM Analyses

SEM micrographs of the unetched surfaces of PLA and PLA/OMMT are displayed in Figures 3(a, b), respectively. As can be observed from Figure 3(a), PLA exhibits a typical fractured surface of a brittle material with rather a smooth surface with no plastic deformation. Few straight parallel lines of crack

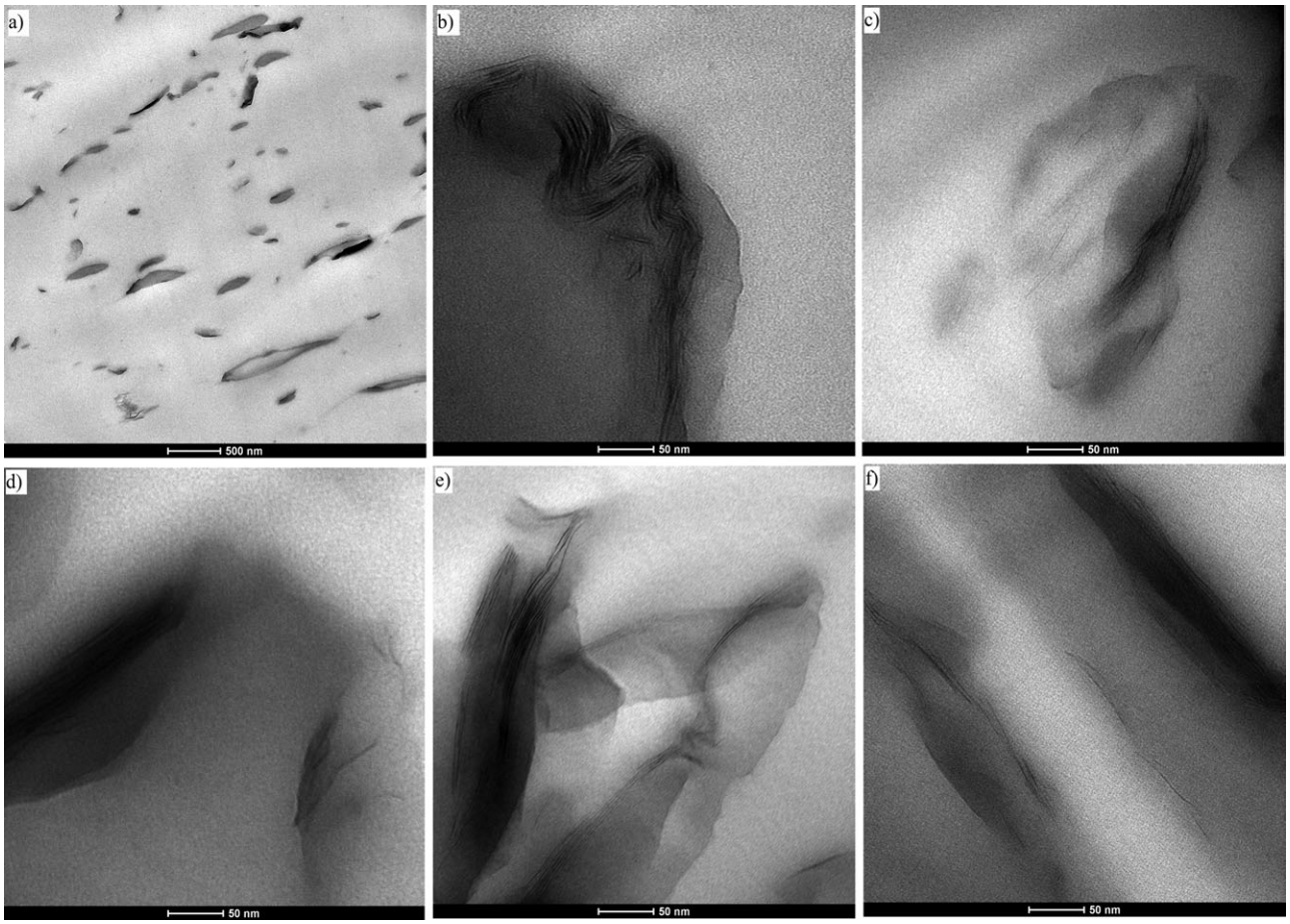

Figure 2. TEM micrographs of the nanocomposites containing 2 wt % clay: (a) PLA/OMMT (500 nm), (b) PLA/OMMT (50 nm), (c) PLA/OMMT/R10 (50 nm), (d) PLA/OMMT/R15 (50 nm), (e) PLA/OMMT/R20 (50 nm), (f) PLA/OMMT/R30 (50 nm). (The R indicates the rubber, and the number following *R* indicates the wt % of the rubber).

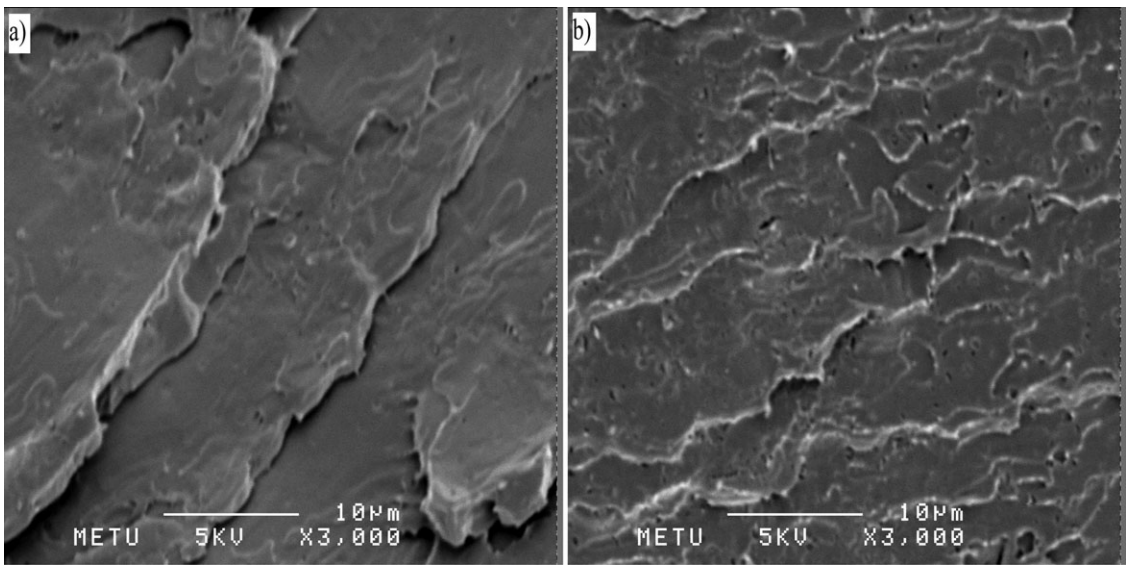

Figure 3. SEM micrographs of the fractured surfaces of the unetched injection molded specimens of (a) PLA and (b) PLA/2 wt % OMMT.

Applied Polymer SCIENCE

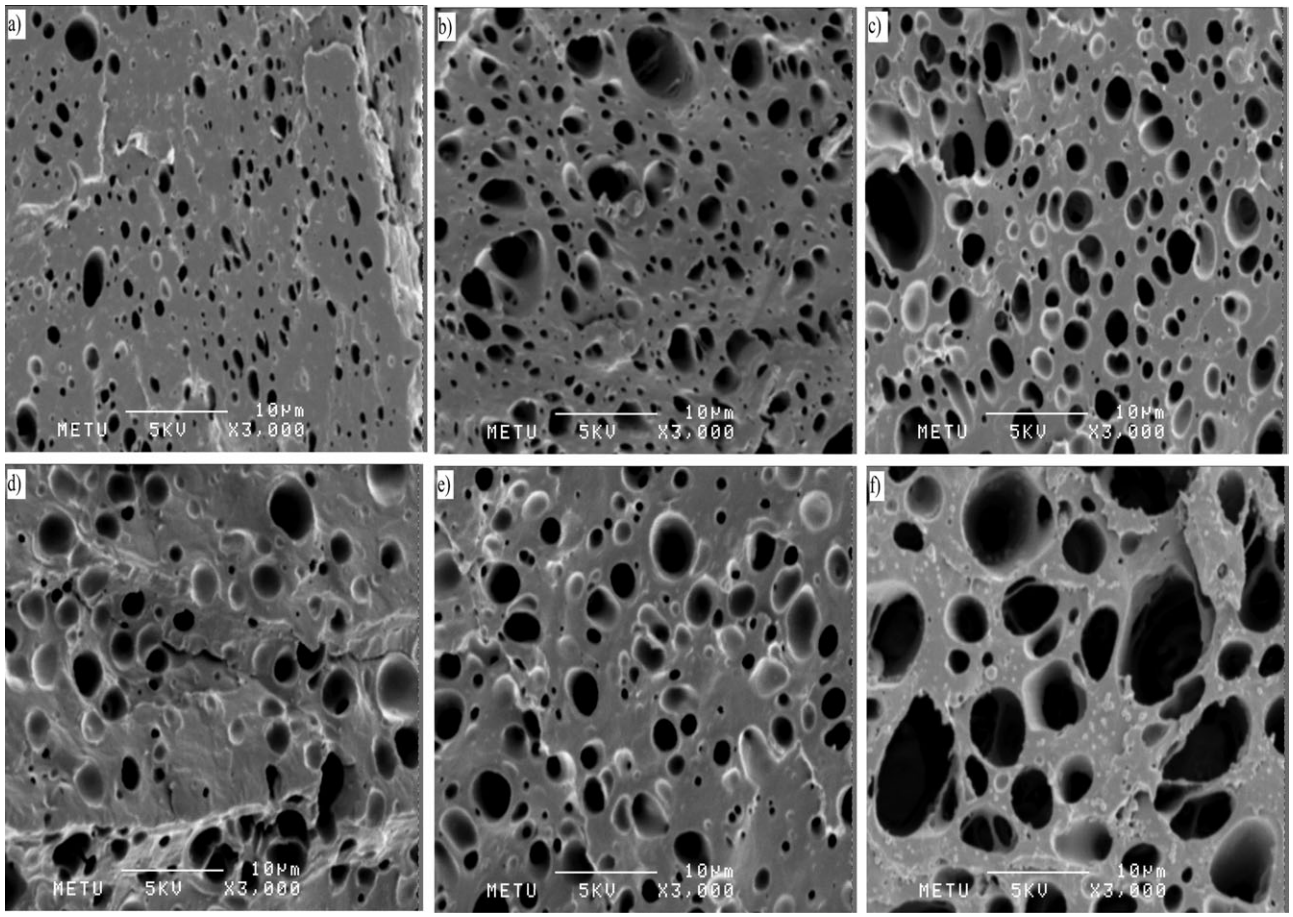

Figure 4. SEM micrographs of the fractured etched surfaces of the injection molded specimens of the binary blends (a–c) and the ternary nanocomposites (d–f) at 10, 20, and 30 wt % rubber content.

propagation are clearly noticeable with no deviations of the cracks implying easy crack initiation and propagation and rapid progress of catastrophic cracks responsible for premature fracture with low energy dissipation.[15,24] PLA/OMMT micrograph shows a rougher fractured surface with multiple small and long crack lines developed in different directions due to the presence of the clay [Figure 3(b)]. This suggests that clay particles deflected the cracks and increased their path. This mechanism that is responsible for roughness and low energy absorption before failure was also observed in Reference12 for PLA/OMMT. The SEM observations of these materials are consistent with the low impact strength and toughness results obtained in mechanical characterization.

Figure 4(a–c) shows typical SEM images of the etched surfaces of the binary blends of PLA/rubber. The vacuoles left after etching reflect the morphology of the dispersed phase. The morphology of the mixtures is that of a two-phase binary blend where PLA formed the continuous phase and the rubber was segregated as spherical domains typical of an immiscible blend, supporting the DSC results discussed later. The rubber particles are evenly dispersed at all concentrations used with narrow size distribution. Their sub-micron mean size (0.4 µm-0.8 µm) suggests low interfacial tension owing to the efficient reaction during compounding between the epoxy groups of the rubber and the hydroxyl and carboxyl terminal groups of the PLA,[1,4,28,31] as well as other possible polar interactions between the ester groups of PLA and those of rubber. Such reaction was proved by Fourier transform infrared spectroscopy by Su et al.[1] in their study of blends of PLA and glycidyl methacrylate grafted poly(ethylene octane) (PLA/mPOE). As also observed in Figure 4(a–c) the domain size increased with increasing rubber content. The viscosity of the dispersed phase increased with increasing rubber content, consequently the droplet coalescence rate increased at the expense of the droplet break up rate, thus large particles were formed.[4] The craters observed are deformed and shaped like ellipsoids with irregular surfaces indicating that the rubber phase shared the impact load with the matrix and was tightly bonded to the PLA. This might also be ascribed to the reaction between the PLA functional groups and the reactive groups of the rubber as mentioned earlier. The copolymer formed at the interface leads to better spatial distribution of the dispersed phase and plays the role of an emulsifier by reducing interfacial tension. Thus, the droplet breakup rate is increased and phase coalescence rate is retarded during melt compounding, consequently small particle size is generated.[4] This copolymer is also efficient in bridging the two components of the blend for efficient load transfer responsible for toughness improvement that is consistent with the results of the mechanical properties.[34] The function of the rubber domains is not only

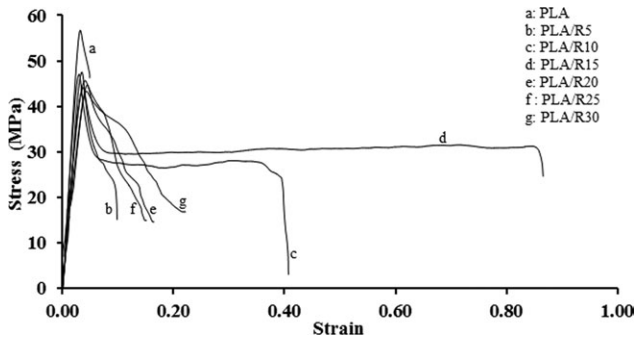

Figure 5. Typical stress–strain curves of the binary blends.

to share the load with the matrix, but to contribute to energy dissipation by initiating multiple crazing in the matrix and to stop and/or divert cracks to prevent their development to rapid catastrophic cracks.[27] Few cracks are also visible in Figure 4(a) with tortuous path due to the presence of the rubber. This indicates that the rubber domains were able to deflect the propagation of the cracks, and the long crack propagation paths absorbed considerable energy contributing to energy dissipation that is responsible for toughness improvement.

Figure 4(d–f) displays the morphology of the ternary nanocomposites. The observed craters had the same morphological features as those of the binary compounds suggesting that the clay did not interfere with the reaction between the rubber and the PLA, but influenced the size of the rubber domains. As observed in these figures, the mean domain size of the nanocomposites increased with increasing rubber content (0.4–1.5 μm) and was mostly larger than that of the binary blends (0.4–0.8 μm). The higher domain size in the nanocomposites suggests that the clay particles did not act as barriers for coalescence, but enlarged the rubber phase domains by affecting the viscosity ratio between the rubber and PLA matrix.[32,34,35]

Mechanical Properties

In general, rubber toughening of polymers leads to reduced strength and stiffness and enhanced toughness provided that a strong interface exists between the phases. However, addition of rigid nanofillers into polymers to form nanocomposites increases strength and stiffness, but may decrease toughness.

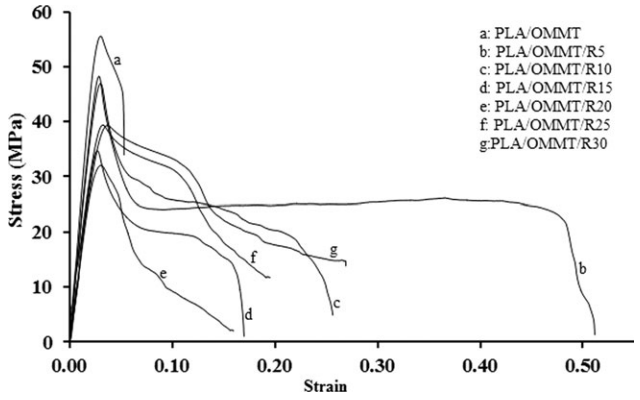

Figure 6. Typical stress–strain curves of the nanocomposites.

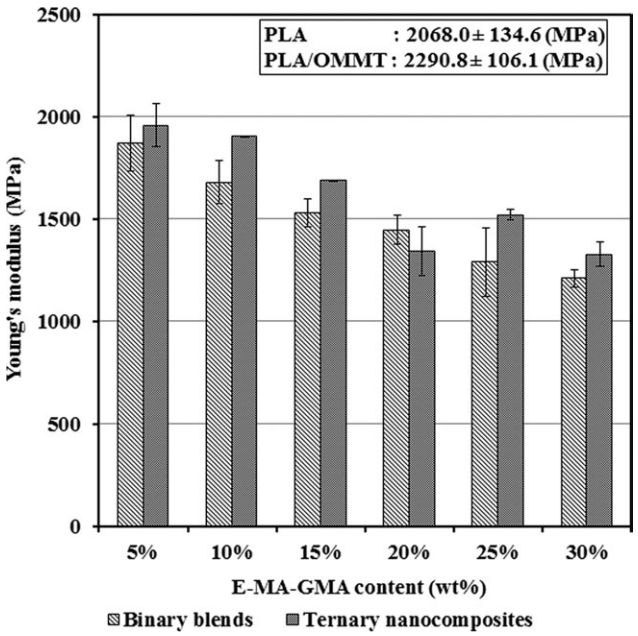

Figure 7. Effect of the rubber content on the Young's modulus of the binary blends and ternary nanocomposites at 2 wt % clay.

Combining the two techniques may lead to balanced properties or even to simultaneous improvement in all the three properties.[35,36] It is reported that in both polymer blends and nanocomposites, the interfacial interactions and the level of dispersion of the components are the key factors that govern the final properties.[34]

Figures 5 and 6 display typical stress–strain curves of pristine PLA, and its binary blends and ternary nanocomposites, and Figures 7–9 show the effect of the rubber and the OMMT on

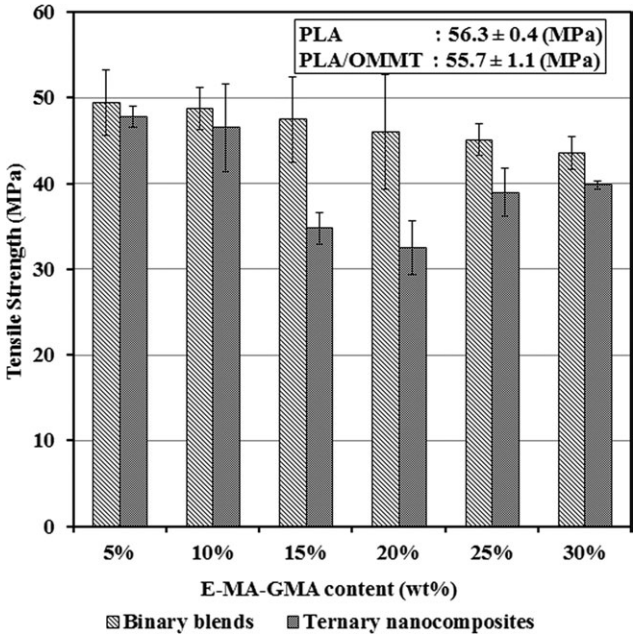

Figure 8. Effect of the rubber content on the tensile strength of the binary blends and ternary nanocomposites at 2 wt % clay.

Applied Polymer SCIENCE

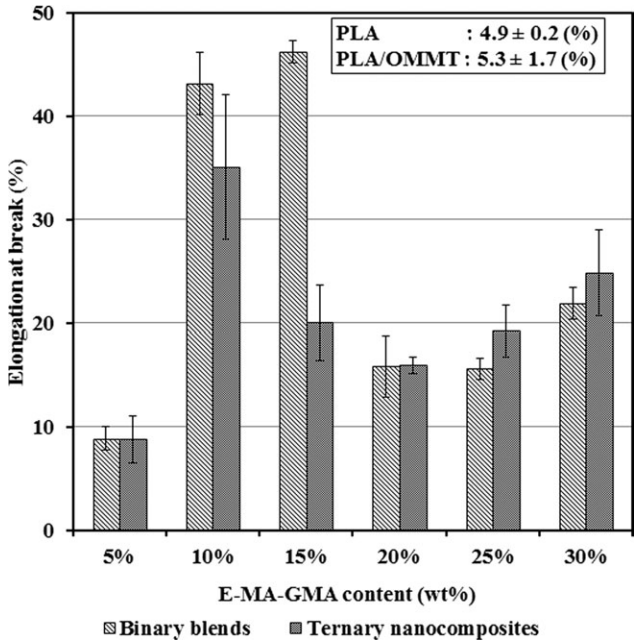

Figure 9. Effect of the rubber content on the elongation at break of the binary blends and ternary nanocomposites at 2 wt % clay.

Young's modulus, tensile strength and elongation at break of these materials respectively.

As can be observed in Figure 5, PLA shows the behavior of a typical rigid and brittle material. During stretching, PLA deformed with a steep linear increase in stress, followed by a yield point and a very short necking. Finally, it fractured catastrophically at very low elongation (ca. 5%) due to lack of crack deviation and cavitation mechanisms as reported by He et al.[37] Slight stress-whitening were visible on specimens indicating that PLA deformed by crazing mechanism.[25] PLA deformation behavior was not significantly affected by the addition of 2 wt % OMMT, and the same mode of deformation was observed. However, more stress-whitening was noticed after the failure of PLA/OMMT. Addition of the rubber induced a substantial change in the tensile behavior of PLA (Figure 5). The failure mode changed from brittle to ductile with a noticeable yield point, longer necking and increased plastic deformation followed by stress softening before failure. All of the stress–strain curves of the binary blends (Figure 5) and nanocomposites (Figure 6) exhibited the same pattern.

Young's Modulus

Addition of 2 wt % organoclay resulted in increase of the tensile modulus of PLA from 2068.0 MPa to 2290.8 MPa (Figure 7). The enhancement in modulus with the addition of OMMT corroborates with the results of other research studies.[2,15,20,29,32] The increase in tensile modulus may be ascribed to the stiffening effect of the dispersed rigid clay layers, as well as the reduced chain mobility of PLA by the surface of the clay.[2,15,20,29] The intercalated/exfoliated structure of the OMMT results in high contact surface area favorable for enhanced interfacial interactions between the carboxyl end groups of PLA and the hydroxyl groups on the organoclay and contributes to chain immobilization.[15,20,29] These interactions are responsible for enhanced adhesion between the PLA matrix and the filler. As a result, an effective stress transfer from the matrix to the filler is established leading to increased elastic modulus.[20]

In the binary blends the modulus dropped steadily as the rubber content is increased (Figure 7) owing to the elastomeric nature of the rubber with low modulus.[2,32,37] The decrease in the modulus was in the range of 10–40% in the composition interval studied. For example, at 20 wt % rubber content, the decrease is around 26% which is lower than the 31% reduction reported for the PLA/poly(ethylene-glycidyl-methacrylate) (PLA/EGMA) blend.[28] This might be ascribed to the presence of methyl acrylate groups in the rubber of the present study. Compared to other findings, the reduction in modulus is similar to the 25% decrease obtained in PLA/NR-*g*-PBA blend,[27] but far less than the 50% decrease in PLA/TPO blend containing 5 phr TPO-PLA as compatibilizer.[30]

In Figure 7 it can be observed that incorporation of 2 wt % OMMT induced a substantial increase in the modulus for all the nanocomposites owing to the stiffening effect of the OMMT that induced chain immobilization as discussed for the PLA/OMMT nanocomposite.[2,15,20,29,32]

Tensile Strength

Figure 8 shows the tensile strength of the blends and nanocomposites. A slight decrease in the tensile strength from 56.3 to 55.7 MPa was observed after addition of 2 wt % OMMT to PLA. In the binary blends, the tensile strength decreased from 49.4 to 43.5 MPa as the rubber content increased from 5 to 30 wt % owing to the elastomeric nature of the rubber.[1,15,29] It should be noted that the tensile strength was affected less by the rubber than the elastic modulus was. The addition of the OMMT to the binary blends also decreased the tensile strength of the binary blends. Similar decrease in tensile strength was observed in a recent study of PLA/SEBS-g-MAH/OMMT nanocomposites.[29] The OMMT counteracted the negative effect of the rubber on the tensile strength only when the rubber content was less than 15 wt % owing to its low content (2 wt %).

Elongation at Break

PLA is a hard and brittle material reported to elongate not more than 10%.[3] Figure 9 shows the effect of the rubber on PLA and its binary blends and ternary nanocomposites. As expected, the elongation at break of pure PLA was very low (≈5%) owing to its rigid nature.

Addition of 2 wt % OMMT did not significantly affect the elongation at break of the PLA, but induced stress whitening upon extension.

Addition of the rubber up to 15 wt% increased the elongation at break of the blends to reach a maximum value of 46% representing 9-fold increase in comparison to that of pristine PLA. Thus, the rubber changed the deformation of PLA from brittle to ductile. This implies that high energy was dissipated during crack propagation before failure owing to the elastic nature of the rubber and to the strong interface developed through the interactions of the ester groups of the rubber and PLA, and the reaction of the epoxy groups of the dispersed rubber phase and

hydroxyl and carboxyl end groups of the PLA matrix leading to the formation of PLA-*g*-rubber at the interface.[2] In addition, this copolymer might have reduced the stress concentration around the dispersed rubber particles by local plastic deformation favorable for increased elongation at break.[15] Beyond 15 wt % rubber content, the elongation at break underwent a drastic reduction and attained a value of ~16% in the range of 20–25 wt % rubber loading. This may be attributed to chain entanglements formed at the interface that might have reduced the chain mobility.[38] Beyond 25 wt % rubber, the elongation at break increased due to high rubber fraction.

The elongation at break of the ternary nanocomposites exhibited the same trend as that of the binary blends. Up to 20 wt % rubber loading, the values of elongation at break of the ternary nanocomposites were lower than those of the binary compositions, due to the constraining effect of OMMT on the molecular mobility.[20,29] Beyond this rubber content, the elongation at break increased owing to higher rubber content.

Impact Strength

Notched impact strength is a measure of the energy necessary to propagate an existing notch (resistance to crack propagation), while unnotched impact strength is a measure of the energy to initiate and propagate a crack (resistance to crack initiation and propagation).[39]

Rubbers containing glycidyl moieties were generally used as impact modifiers and/or as compatibilizers with different success.[2,4,28,40] In rubber toughened polymer blends numerous factors such as the extent of mixing, rubber content, viscosity ratio, interfacial adhesion, and rubber particle size affect the final morphology and hence the final properties.[23,24]

The effects of the OMMT and the rubber on notched Charpy impact strength (IS) of neat PLA are reported in Figure 10. PLA subjected to impact load failed in a brittle manner typical of a glassy polymer and the low impact strength recorded was only 3.2 KJ/m^2. Broken specimens showed intense stress whitening especially near the notch tip characteristic of local crazing. The incorporation of the clay imparted a negligible decrease (≈3%) in the IS of plain PLA which is within the experimental error. Similar results were obtained for nylon-clay nanocomposites.[41] The IS was maintained relatively constant owing to the efficient interactions between PLA and the OMMT and to the intercalation/exfoliation as revealed by XRD and TEM. However, no improvement could be obtained owing to the absence of deformation mechanisms to absorb and dissipate energy such as crazing, cavitation and shear yielding.[15]

The addition of the rubber significantly enhanced the impact strength of the PLA. The IS increased steadily from 4 KJ/m^2 at 5 wt % rubber content to reach a maximum of 9.5 KJ/m^2 at 30 wt % rubber content. This is attributed to the elastomeric nature of the rubber and its fine and homogeneous dispersion, as well as to the strong interface developed during compounding as discussed earlier.[4,15] The reactions led to the formation of a grafted copolymer (PLA-*g*-rubber) located at the interface that acted as an emulsifier and reduced the interfacial tension between the two phases resulting in high level of dispersion,

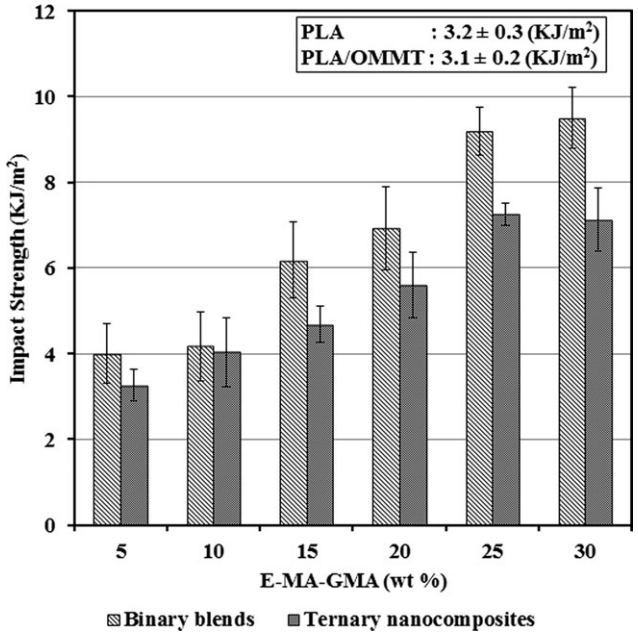

Figure 10. Effect of the rubber content on the notched Charpy impact strength of the binary blends and ternary nanocomposites at 2 wt % clay.

fine particle size, and low polydispersity as observed by SEM. The rubber inclusions acted as stress concentrators during impact deformation and transformed the behavior of the PLA from brittle to ductile by changing the mechanism of deformation. Such mechanisms of deformation might include crazing, cavitation, shear bending, crack bridging and shear yielding that are well known in toughened polymer blends.[2]

At 10 wt % rubber content, the binary blend and the ternary nanocomposite exhibited nearly the same IS value, probably due to the highest exfoliation state observed in this nanocomposite. At other rubber contents, the IS values of the ternary nanocomposites were lower than those of the corresponding binary blends. This could be attributed to their larger particle size (0.4–1.5 μm). It was reported that well dispersion of clay into a blend might suppress coalescence.[32] However, the opposite result was obtained in the present study that might indicate that most of the clay was encapsulated in the rubber phase with some clay residing at the interface between the PLA and the rubber and in the PLA matrix as discussed earlier in the XRD and TEM sections. Yu et al.[42] reported that high toughness is obtained when maximum quantity of exfoliated clay is dispersed in the continuous phase of a functionalized rubber toughened blend. In conclusion, in this study, the organoclay was more effective for improvement of modulus than for improvement of impact toughness. At 2 wt % OMMT, balanced stiffness-toughness was observed at 10 wt % rubber content that exhibited the highest level of exfoliation.

Melt Flow Index Measurements

Rheological measurements are widely used as a mean to determine the extent of interactions in reactive polyblends.[15,37] The rheological properties of the pristine materials, the blends and the nanocomposites were determined using melt flow index measurements (MFI).

Applied Polymer SCIENCE

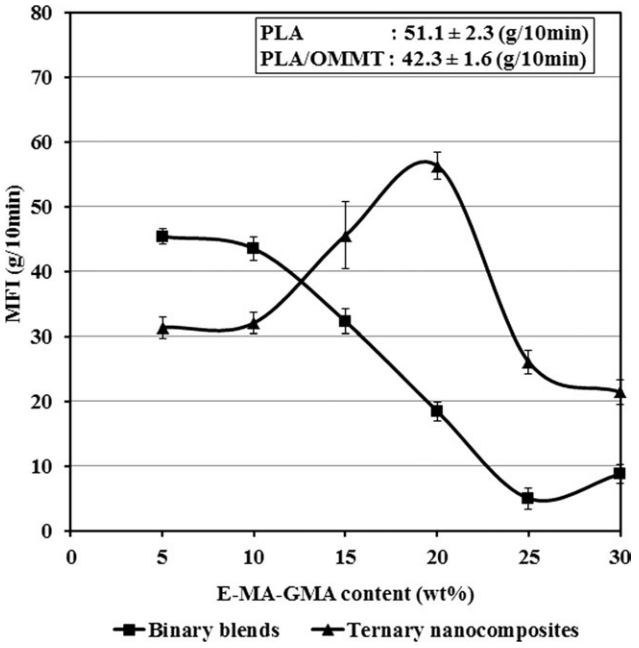

Figure 11. Effect of the rubber content on the MFI of the binary blends and ternary nanocomposites at 2 wt % clay.

Figure 11 shows the MFI of the starting materials and the compounds. The MFI of the injection grade PLA increased from 47.2 to 51.1 g/10 min after extrusion indicating that its molecular weight has been decreased as expected, since PLA is known to be a shear sensitive material.[13]

Addition of 2 wt % clay to PLA decreased the MFI to 42.3 g/10 min. The decrease in the MFI (increase in viscosity) is attributed to the "filler effect," as well as to the enhanced interactions of the modified clay and the PLA through possible interactions of the carboxyl and hydroxyl terminal groups of the PLA with the hydroxyl groups of the surfactant of the clay that constrain chain mobility.[15,20] Also, the aspect ratio of clay increases through delamination of the clay agglomerates and exfoliation as observed by XRD and TEM giving rise to larger surface area for interactions that restrict the flowability of the material.[20]

In the binary blends of PLA/rubber, addition of the rubber up to 25 wt % to PLA decreased the MFI. The decrease in MFI is attributed to the high viscosity of the rubber and to the reaction of the epoxy groups of the rubber with the hydroxyl and carboxyl end groups of the PLA and the likely polar interactions of their ester groups. The reaction might lead to formation of a graft copolymer at the PLA and the rubber interface that would strengthen the interfacial adhesion, restrict chain mobility, and reduce slippage of the chains at the interface.[15,20] In the literature, interfacial interactions are reported to result in increase in viscosity (decrease in MFI) in several polymer systems.[1,29,30] For example, Kusmono et al.[15] reported a decrease in MFI after addition of SEBS-*g*-MAH to compatibilize a PA6/PP blend. They attributed such a decrease to the formation of SEBS-*g*-PA6 copolymer at the interface due to reaction of PA6 amine groups with maleic anhydride groups of SEBS-MAH. At 30 wt % rubber content, the MFI of the blend increased to reach approximately the MFI of the neat rubber measured as 8.3 g/10 min.

In the ternary nanocomposites, the MFI increased up to the composition containing 20 wt % of rubber. This increase might be due to plasticizing effect of the dissolved clay surfactant. As the viscous rubber content is increased, more of the clay platelets are delaminated and some of the surfactant of the clay dissolves in the matrix inducing plasticization and increasing the MFI.[13,20] At even higher rubber contents, the plasticization effect of the clay surfactant was hindered by the high content of the highly viscous rubber, consequently the MFI decreased.

Thermal Properties

Differential Scanning Calorimetry was performed from room temperature to 220°C using samples from tensile injected dogbones to evaluate the effects of the organoclay and the rubber on the phase transition behavior of the PLA and the mixtures. Thermograms of PLA and its binary blends and ternary nanocomposites exhibited three main transitions namely: a glass transition temperature (T_g), a crystallization exotherm (characterized by T_c and ΔH_c), and a melting endotherm (characterized by T_m and ΔH_m). Table I summarizes the values of these calorimetric parameters and the degree of crystallization of PLA calculated from eq. (1) using a value of 93 J/g for the heat of fusion of 100% crystalline PLA.[24,27,28]

The melting temperature of the rubber was recorded as 53.1°C, and its glass transition temperature that is below room temperature was not studied here. The thermogram of pure PLA is characterized by a glass transition temperature at 58.9°C, a crystallization exotherm at $T_c = 118.2$°C, and a melting endotherm at $T_m = 152.7$°C (Table I). As shown in this table, and considering the experimental error of the measurements, PLA in the binary blends and ternary nanocomposites exhibited the same glass transition temperature as the pure PLA, suggesting that PLA and the rubber were immiscible in the composition range studied. Similarly, Ishida et al. studied toughening of PLA with different types of rubbers, and the DSC thermograms of all the blends exhibited a single glass transition temperature, thus it was concluded that the compounds were immiscible.[23]

In the binary blends, the addition of the rubber had no significant effect on the melting temperature of the PLA. This suggests that the incorporation of the rubber did not change the crystal structure of PLA as also observed by Zeng et al.[3] On the other hand, the crystallization temperature decreased substantially, after addition of only 5 wt % of rubber, and it dropped from 118.2 to 109.5°C due to the nucleating effect of the rubber that favors initiation and crystal growth at many sites. In a recent study, Petchwattana et al.[24] reported that addition of only 0.5 wt % ultrafine acrylate rubber did not affect the melting temperature of PLA, but it decreased the crystallization temperature. This result was attributed to the rubber particles that might have acted as nucleating sites for crystallization. It was also found that further increase of the rubber content inhibited crystallization. Oyama[28] reported that the dispersed poly(ethylene-glycidyl-methacrylate) rubber (EGMA) in PLA played the role of nucleating agent and promoted the crystallization of PLA, and further annealing of the blends for 2.5 h at 90°C

Table I. Thermal Parameters of PLA, the Binary Blends and the Nanocomposites

Sample	T_g (°C)	T_c (°C)	$\triangle H_c$ (J/g)	T_m (°C)	$\triangle H_m$ (J/g)	W_c (%)
Thermal parameters of PLA and the binary blends						
PLA	58.9	118.2	20.2	152.7	25.6	5.8
PLA/R5	57.3	109.5	23.3	152.4	27.7	5.0
PLA/R10	57.4	108.4	19.8	152.8	24.4	5.5
PLA/R15	57.6	107.8	19.4	152.6	24.9	6.9
PLA/R20	57.5	106.5	15.9	152.1	23.9	10.8
PLA/R25	57.9	108.2	13.8	152.2	22.4	12.3
PLA/R30	58.1	109.3	13.6	151.9	21.3	11.8
Thermal parameters of PLA and the nanocomposites						
PLA	58.9	118.2	20.2	152.7	25.6	5.8
PLA/OMMT	57.5	107.6	23.2	151.7	26.2	3.3
PLA/OMMT/R5	57.0	109.7	21.3	151.9	26.6	6.1
PLA/OMMT/R10	57.7	105.2	17.1	151.8	25.6	10.4
PLA/OMMT/R15	57.8	103.2	16.5	151.1	23.1	8.6
PLA/OMMT/R20	58.5	104.9	15.9	151.3	20.4	6.3
PLA/OMMT/R25	58.5	105.5	14.4	151.4	19.8	8.0
PLA/OMMT/R30	58.1	108.8	14.4	151.2	19.2	7.6

resulted in super-tough PLA blends. Table I shows that in general the degree of crystallization of the binary blends increased with higher rubber loading, possibly due to the chemical reaction between the epoxy groups of the rubber and the carboxyl and hydroxyl terminal groups of PLA and the likely polar interactions of their ester groups that increased the viscosity of the system. According to Oyama,[28] the high viscosity causes a high shear force during mixing and pulls out the copolymer formed by the reaction of PLA and EGMA at the interface, to the PLA matrix. In the present study, it is thought that this phenomenon has also occurred in our PLA based blends and the pull out of the copolymer from the interface to the bulk of the matrix induced the chain mobility necessary for crystallization, thus the degree of crystallization increased.

Table I indicates that the incorporation of 2 wt % OMMT into PLA did not significantly affect the melting temperature and glass transition temperature of PLA as also found by Chow et al.[16] On the other hand, the crystallization temperature was drastically decreased from 118.2 to 107.6°C. This is ascribed to the nucleation effect of the clay owing to its large surface area.[20,29] The intercalated/exfoliated structure as observed by XRD and TEM could also have contributed to the increase in the nucleating sites as reported by Balakrishnan et al.[20] Similar results were also reported by other research groups.[12,16] The degree of crystallinity of PLA/OMMT was lower than that of the neat PLA. This might be due to the hindrance caused by exfoliated/intercalated structure of the organoclay that reduced the mobility of polymer chains.[15,29]

The crystallization temperatures of the ternary nanocomposites are generally lower in comparison to the crystallization temperatures of the binary blends that have the same quantity of rubber (Table I). This is also attributed to the nucleating effect of the nanofiller.[20,29] In the ternary nanocomposites with 5–10 wt % rubber, the viscosity increased (MFI decreased) in comparison to that of PLA/OMMT as shown in Figure 11. The degree of crystallization increased owing to the effect described by Oyama[28] overcoming the hindrance effect of the clay. In the ternary nanocomposites with 15–20 wt % rubber, the viscosity decreased (Figure 11), thus the chain mobility is expected to be enhanced. However, in this range, the degree of crystallization decreased that might be attributed to immobilization of the polymer molecules by clay. In the ternary nanocomposites with 20–30 wt % of rubber, the degree of crystallization levels up owing to high viscosity and the constraining effect of the clay. Both of these factors reduce chain mobility needed for crystallization. The effect described by Oyama[28] did not take place at this high level of rubber content possibly due to saturation of the interface corresponding to maximum interactions.[39]

CONCLUSIONS

PLA was successfully toughened by melt blending with E-MA-GMA rubber in the range of 5 to 30 wt % using a twin screw extruder. Organoclay was added at 2 wt % to compensate the decrease in other mechanical properties. XRD and TEM showed that PLA/OMMT binary nanocomposite exhibited intercalated/exfoliated structure with some remaining tactoids. Addition of the rubber promoted dispersion of the OMMT by intercalating with PLA molecules into the clay galleries. At 10 wt % rubber content exfoliation was observed. Beyond this rubber content, intercalated/exfoliated structure reappeared and no further enhancement in dispersion was observed.

The morphology revealed by SEM showed that PLA and E-MA-GMA were immiscible in the range of rubber content studied, and the rubber formed the dispersed phase. The addition of rubber changed the brittle behavior of PLA to ductile by inducing debonding and/or cavitation. The rubber domain size increased with increasing rubber content in both the blends and

nanocomposites. The nanocomposites exhibited coarser morphology suggesting that the clay did not act as a barrier for the coalescence owing to its likely preferential location in the rubber.

The impact strength and the elongation at break were improved in the binary blends and ternary nanocomposites at the expense of stiffness and strength. In the ternary nanocomposites, the best balance of these properties was observed at 10 wt % rubber content.

The viscosity of the blends and nanocomposites, evaluated by MFI measurements, was highly influenced by the rubber and the clay. The MFI of the binary blends decreased with increasing rubber content up to 25 wt % rubber. In the ternary nanocomposites, an increase of the MFI was observed up to 20 wt % rubber content owing to the plasticization effect of the dissolved organoclay surfactant, and beyond this rubber content, the MFI decreased owing to the highly viscous rubber content.

DSC analysis showed that the T_g of PLA in the blends and nanocomposites was not significantly influenced by the presence of the rubber confirming the immiscibility of the mixtures. Both the clay and the rubber decreased the crystallization temperature of PLA and acted as nucleating agents for PLA and affected its crystallization.

REFERENCES

1. Su, Z.; Li, Q.; Liu, Y.; Hu, G.; Wu, C. *Eur. Polym. J.* **2009,** *45*, 2428.
2. Kumar, M.; Mohanty, S.; Nayak, S. K.; Parvaiz, M. R. *Biores. Techn.* **2010,** *101*, 8406.
3. Zeng, J.; Li, Y.; He, Y.; Li, S.; Wang, Y. *Ind. Eng. Chem. Res.* **2011,** *50*, 6124.
4. Sun, S.; Zhang, M.; Zhang, H.; Zhang, X. *J. Appl. Polym. Sci.* **2011,** *122*, 2992.
5. Liu, H.; Zhang, Z. *J. Polym. Sci. Part B: Polym. Phys.* **2011,** *49*, 1051.
6. Meng, B.; Tao, J.; Deng, J.; Wu, Z.; Yang, M. *Mater. Lett.* **2011,** *65*, 729.
7. Ljungberg, N.; Andersson, T.; Wesslén, B. *J. Appl. Polym. Sci.* **2003,** *88*, 3239.
8. Martino, V. P.; Jiménez, A.; Ruseckaite, R. A. *J. Appl. Polym. Sci.* **2009,** *112*, 2010.
9. McManus, A. J.; Doremus, R.; Siegel, R.; Bizios, R. *J. Biomed. Mater. Res. A* **2005,** *72*, 98.
10. Kasuga, T.; Maeda, H.; Kato, K.; Nogami, M.; Hata, I.; Ueda M. *Biomaterials* **2003,** *24*, 3247.
11. Kasuga, T.; Ota, Y.; Nogami, M.; Abe, Y. *Biomaterials* **2001,** *22*, 19.
12. Marras, S. I.; Zuburtikudis, I.; Panayiotou, C. *Eur. Polym. J.* **2007,** *43*, 2191.
13. Carrascoa, F.; Gamez-Perez, J.; Santanac, O. O.; Maspoch, M. L. L. *Chem. Eng. J.* **2011,** *178*, 451.
14. Chow, W. S.; Lok, S. K. *J. Thermo. Comp. Mater.* **2008,** *21*, 265.
15. Kusmono; Ishak, Z.; Chow, W. S.; Takeichi, T.; *Rochmadi. Euro. Polym. J.***2008,** *44*, 1023.
16. Chow, W. S.; Lok, S. K. *J. Therm. Calorim.* **2009,** *95*, 627.
17. Chang, J. H.; An, Y. U.; Cho, D.; Giannelis, E. P. *Polymer* **2003,** *44*, 3715.
18. Yokohara, T.; Yamaguchi, M. *Eur. Polym. J.* **2008,** *44*, 677.
19. Broz, M. E.; VanderHart, D. L.; Washburn, N. R. *Biomaterials* **2003,** *24*, 4181.
20. Balakrishnan, H.; Hassan, A.; Wahit, M. U.; Yussuf, A. A.; Abdul Razak, S. B. *Mater. Des.* **2010,** *31*, 3289.
21. Lee, J. B.; Lee, Y. K.; Choi, G. D.; Na, S. W.; Park, T. S.; Kim, W. N. *Polym. Degrad. Stab.* **2011,** *96*, 553.
22. Nijenhuis, A. J.; Colstee, E.; Grijpma, D. W.; Pennings, A. *J. Polymer* **1996,** *37*, 5849.
23. Ishida, S.; Nagasaki, R.; Chino, K.; Dong, T.; Inoue, T. *J. Appl. Polym. Sci.* **2009,** *113*, 558.
24. Petchwattana, N.; Covavisaruch, S.; Euapanthasate, N. *Mater Sci. Eng. A* **2012,** *532*, 64.
25. Theryo, G.; Jing, F.; Pitet, L. M.; Hillmyer, M. A. *Macromolecules* **2010,** *43*, 7394.
26. Li, Y.; Shimizu, H. *Macromol. Biosci.* **2007,** *7*, 921.
27. Zhang, C.; Man, C.; Pan, Y.; Wang, W.; Jiang, L.; Dan, Y. *Polym. Int.* **2011,** *60*, 1548.
28. Oyama, H. T. *Polymer* **2009,** *50*, 747.
29. Leu, Y. Y.; Mohd Ishak, Z. A.; Chow, W. S. *J. Appl. Polym. Sci.* **2012,** *124*, 1200.
30. Ho, C.; Wang, C.; Lin, C.; Lee, Y. *Polymer* **2008,** *49*, 3902.
31. Hashima, K.; Nishitsuji, S.; Inoue, T. *Polymer* **2010,** *51*, 3934.
32. Bitinis, N.; Verdejo, R.; Maya, E. M.; Espuche, E.; Cassagnau, P.; Lopez-Manchado, M. A. *Comp. Sci. Tech.* **2012,** *72*, 305.
33. Abramoff, M. D.; Magalhaes, P. J.; Ram, S. *J. Biophotonics Int.* **2004,** *11*, 36.
34. Yeniova, C.; Yilmazer, U. *Polym. Comp.* **2010,** *31*, 1853.
35. Martins, C. G.; Larocca, N. M.; Paul, D. R.; Pessan, L. A. *Polymer* **2009,** *50*, 1743.
36. Alyamac, E.; Yilmazer, U. *Polym. Comp.* **2007,** *28*, 251.
37. He, S.; Wu, W.; Wang, R.; Pu, W.; Chen, Y. *Polym.-Plast. Technol. Eng.* **2011,** *50*, 719.
38. Chow, W. S.; Neoh, S. S. *Polym.-Plast. Technol. Eng.* **2010,** *49*, 62.
39. Baouz, T.; Fellahi, S. *J. Appl. Polym. Sci.* **2005,** *98*, 1748.
40. Coskunses, F. I.; Yilmazer, U. *J. Appl. Polym. Sci.* **2011,** *120*, 3087.
41. Okada, A. *Mater. Sci. Eng. C* **1995,** *3*, 109.
42. Yu, Z. Z.; Hu, G. H.; Varlet, J.; Dasari, A.; Mai, Y. W. *J. Polym. Sci. Part. B: Polym. Phys.* **2005,** *43*, 1100.